Radiomics for Differentiation of the Posterior Fossa Pilocytic Astrocytoma Versus Hemangioblastomas in Adults. A Pilot Study

Houman Sotoudeh (hsotoudeh@uabmc.edu)
The University of Alabama at Birmingham School of Medicine https://orcid.org/0000-0002-5510-7062
Zahra Saadatpour
The University of Alabama at Birmingham Department of Radiology
Ali Rezaei
The University of Alabama at Birmingham Department of Radiology
Mahsan Sotoudeh
Islamic Azad University Arak Branch
Charles A Wheeler
The University of Alabama at Birmingham Department of Radiology
Aparna Singhal
The University of Alabama at Birmingham Department of Radiology
Manoj Tanwar
The University of Alabama at Birmingham Department of Radiology

Research Article

Keywords: Pilocytic Astrocytoma, hemangioblastoma, Artificial Intelligence, Magnetic Resonance Imaging

Posted Date: February 7th, 2022

DOI: https://doi.org/10.21203/rs.3.rs-1319236/v1

Abstract

Purpose:

Both pilocytic astrocytoma (PA) and hemangioblastoma (HB) are common primary neoplasms of the posterior fossa with similar radiological manifestations. This study was conducted to evaluate the role of radiomics in differentiating these two conditions in adults.

Materials and Methods:

After a retrospective search of our institutional imaging archive, adult patients with a known diagnosis of PA or HB were included. We reviewed each patient's most recent preoperative brain magnetic resonance imaging (MRI). The solid enhancing nodule of each lesion on post-contrast T1 sequence was manually segmented. Multiple radiomic features were then extracted from each nodule using the Pyradiomic library. Subsequently, the most predictive features were identified by feature selection models. Following this, different machine learning (ML) models were constructed based on these selected features to classify lesions as PA or HB. Finally, we evaluated the performance of each model by leave-one-out cross-validation.

Results:

With inclusion and exclusion criteria, 34 enhancing PA nodules and 39 HB nodules were selected. A total of 115 features were extracted from each enhancing nodule. Twelve characteristics were detected as most predictive of histopathological diagnosis. Among various ML models, the neural network had the best performance in differentiating these two conditions with an AUC of 0.9 and an accuracy of 82%.

Conclusions:

In this retrospective study, radiomic MRI techniques demonstrated high performance in distinguishing adult posterior fossa PA from HB. Future development of radiomic models may advance presurgical diagnosis of these two conditions when added to routine clinical practice and thus improve patient management.

Purpose

According to the WHO classification of central nervous system (CNS) malignancies, pilocytic astrocytoma (PA) and hemangioblastoma (HB) are grade I tumors. PA is the most common neoplasm in the posterior fossa during childhood, usually presenting between 5-13 years of age [1, 2]. PA is a slow-growing neoplasm, and the most common clinical manifestations are secondary to increased intracranial pressure, such as headache, vomiting, vision, and gait disturbance [2]. On the other hand, HB is another grade I, highly vascular neoplasm of the posterior fossa with very similar clinical symptoms. HB can be sporadic or secondary to von Hippel-Lindau (VHL) disease, usually in adults with a mean age of 40-45 years of old [3–6].

The classical magnetic resonance imaging (MRI) characteristics of these two posterior fossa tumors are very similar, demonstrating a cystic lesion with a mural nodule, which typically avidly enhances following the injection of contrast media (Fig. 1) [6]. Traditionally, a cystic lesion in the posterior fossa with an enhancing nodule is reported as a PA if the patient is a teenager and HB if the patient is an adult. However, this approach is not always accurate since some HB occur in children, and some PA happen in older adults. Also, these tumors do not always present with classic radiological findings and may present as a purely cystic lesion or purely solid enhancing nodule [7].

Despite advances in structural imaging, accurate differentiation of these tumor types on imaging remains a challenge for neuroradiologists as well as neuro-oncologists, and definitive diagnosis necessitates histopathological examination. Biopsy with tissue analysis remains the standard for accurate diagnosis. However, surgical intervention can be associated with significant risks, such as post-biopsy hemorrhage, stroke, accidental injury, and perioperative infection. Furthermore, surgical techniques for these two neoplasms can be quite disparate. For instance, the associated cyst in HB is caused by extravasation of plasma from neoplastic vessels with increased permeability and peripheral gliosis [8, 9]. Thus, the surgical technique in HB constitutes resection of the enhancing nodule while leaving the cyst behind [8, 10]. On the other hand, PA in adults is more aggressive than in children, and gross total resection of the entire lesion—including both nodule and cyst—is currently considered standard of care [11–13]. Having an accurate prospective diagnosis can be valuable and significantly affect presurgical planning.

Radiomics is an emerging technique in medical imaging to study finer tumor characteristics. A radiomics pipeline constitutes lesion segmentation on medical imaging (CT, MRI, PET); extraction of multiple features from segmented regions; selection of most predictive features; and construction of different ML models based on these features to predict specific clinical outcomes. The most common application of radiomics has been recognized in the field of oncology with varied success in prediction of tumor histopathology, genetic mutation, and treatment response [14].

In this study, we evaluate the role of radiomics in differentiating between adult PA versus HB on MR imaging.

Material And Methods

The Ethics Committee approved this institutional retrospective study (Record Number IRB-120719006). We evaluated tumor histopathology results of adult patients who underwent surgery for HB or PA at our institution. Electronic medical records (EMR) and imaging data of patients with these diagnoses were analyzed from 2012 to 2021. Only patients with HB and PA in the posterior fossa were selected. The most recent brain MRI before tumor resection was then collected. After reviewing these images, patients with sequelae of prior hemorrhage, surgery, radiation, or other chronic pathology in the posterior fossa such as remote infarction were excluded. Moreover, only patients with nodular enhancement in the posterior fossa were included for final analysis.

After normalization and co-registration on post-contrast T1 sequence of each patient, the enhancing nodule was manually segmented using 3D slicer software [15]. The radiomic features of each segmented nodule were then extracted using the Pyradiomics library [16]. The most predictive features were isolated via information gain analysis and then integrated into ML algorithms. Assorted ML models were developed to differentiate HB from PA. These include AdaBoost, Decision Tree (DT), k-nearest neighbors algorithm (KNN), Neural network (NN), Random Forest (RF), Naive Bayes, and Support Vector Machines (SVM). Post-processing of extracted features, feature selection, and ML modeling were performed using the Orange data mining platform version 3.27 (Bioinformatics Lab at University of Ljubljana, Slovenia) [17]. The performance of each model was then reported by the area under the curve (AUC), accuracy, sensitivity, and specificity via the leave-one-out technique. All statistical analyses were performed using SPSS version 22 (Chicago, IL: SPSS Inc.). A P-value of 0.05 was determined to be the cutoff point for statistical significance. The materials and methods of this study have been summarized in Fig. 2.

Results

After inclusion and exclusion criteria, 34 patients with PA were selected for final analysis, including 11 male and 23 female patients (mean age of 33.44 and a standard deviation of 16.4). A total of 39 hemangioblastomas were included from 18 patients, including 7 males and 11 females (mean age of 38.3 and standard deviation of 11.8). All PA neoplasms were resected. Several patients with Von Hippel Lindau (VHL) syndrome underwent resection for at least one nodule, consisting of biopsy-proven HB. In these patients, other enhancing nodules of the posterior fossa were also considered HB and included in this study. The age of these two patient populations was not significantly different (P-value of 0.22).

114 features were extracted for each enhancing nodule. Upon implementing feature selection (via information gain analysis), 12 most predictive characteristics were identified to build ML models. The selected feature include: Maximum3DDiameter, MajorAxisLength, Sphericity, LeastAxisLength, Maximum2DDiameterSlice, SurfaceArea, Maximum2DDiameterColumn, Maximum2DDiameterRow, Idn, GrayLevelNonUniformity (glrlm), GrayLevelNonUniformity (glszm), and Coarseness.

Among different models, the neural network demonstrated the highest performance (AUC of 0.9), followed by random forest, KNN, SVM, Naive Bayes, AdaBoost, and DT (table 1).

The detailed structure for each model includes KNN (Number of neighbors: 8, Metric: Euclidean, and Weight: Uniform), Decision Tree (Induce binary tree, Minimum number of instances in leave: 9, No split subsets smaller than 8, Maximum tree depth: 100, and Stop when majority reaches: 95%), Random Forest (Number of trees: 30, Replicable training, No split subsets smaller than 9), SVM (Cost: 1.7, Regression loss epsilon: 0.2, Kernel: Sigmoid, Optimization Numerical Tolerance: 0.01, and Optimization Iteration Limit: 100), AdaBoost (Base estimator: Tree, Number of estimators: 57, Learning rate: 1, Classification algorithm: SAMMER, and Regression loss function: Linear), and Neural Network (Neurons in the hidden layers: 100,50,20, Activation: tanh, Solver: Adam, Regularization $\alpha = 0.0001$, and Maximum number of iterations: 300).

Discussion

The cerebellum and majority of the brainstem are located in the posterior fossa, extending from tentorium superiorly to foramen magnum inferiorly, with rarer pathologies than in the supratentorial region [18]. Subacute stroke is the most common lesion with mass effect in the posterior fossa among adults, whereas intra-axial cerebellar metastases and extra-axial vestibular schwannoma are the most prevalent neoplastic lesions. HB is the most common primary intra-axial tumor of the posterior fossa in adults, presenting as a hypervascular enhancing nodule with or without a cyst. Of mesenchymal/meningeal origin, it constitutes 1.0–2.5% of all intracranial neoplasms and arises from embryologic multipotent stem cells (hemangioblasts) with deletion of both *VHL* tumor suppressor genes [19]. 60% of HB present with classic solid nodule and cyst, whereas 40% present with only an enhancing nodule. Mass effect from cyst expansion is considered the main cause of clinical symptoms, given the fact that purely nodular HBs are often asymptomatic [20].

Pilocytic astrocytoma is rare in adults, with an incidence of fewer than 0.1 cases per 100,000 person-years, and often involves the cerebral hemispheres. 27% of adult PAs occur in the cerebellum, 50% are solid with variable enhancement, 29% with mixed solid-cystic, and 21% with classic cyst with an enhancing mural nodule appearance [21].

There are no conventional MRI criteria to differentiate solid enhancing HB from solid enhancing PA, or to differentiate cyst with mural nodule secondary to HB from that of PA. There are several studies investigating advanced MRI to distinguish between these two tumors. In one study of posterior fossa tumors reviewing only 2 PA and 2 HB patients, the ADC values of these two tumors were similar (1.61 $x10^{-3}$ mm^2/s versus 1.7 $x10^{-3}$ mm^2/s) [22].

In the past, ML approaches have been used to differentiate PA from HB. In one study that analyzed 248 patients with intra-axial posterior fossa tumors by ML modeling (including 65 metastases, 27 ependymomas, 26 medulloblastomas, 10 astrocytomas other than PA, 8 lymphomas, 7 atypical teratoid/rhabdoid tumors (ATRT), 6 glioblastomas, 44 HB, and 43 PA), researchers were able to classify them with a 90% accuracy rate. Predictive features in that study were ADC histogram of the solid tumor component, structural MRI findings (tumor location, lesion morphology, enhancement pattern, extension along neuroaxis, T2-FLAIR signal, and mass effect), and patient age. The best ML model was random forest [23]. The aforementioned study included both children and adults with a mean age of 18.7 for PA patients and 57.6 for HB. Given that they utilized age as a predictive feature, their model had a relative advantage in differentiating PA from HB. In our study, all patients were adults without a significant difference in age between the two cohorts. Although our models did not exploit age, our performance remained competitive with an AUC of 90% for the best model. Moreover, the prior study employed manual imaging feature extraction by radiologists, while we utilized software-based automation, which can eliminate inter and intra-observer variability.

Nonetheless, our study has several limitations. Firstly, this retrospective analysis was conducted on a relatively small patient population. PA is not common in adults, leading to a relative paucity of data in our medical databases. Secondly, we only segmented the enhancing tumor component on the T1 post-contrast sequence in this conceptual study. Using other portions of the tumor and additional sequences may lead to better algorithm performance.

Conclusion

Differentiation between HB and PA in the adult posterior fossa is challenging on conventional medical imaging. However, an accurate preoperative diagnosis is crucial and can significantly alter patient management and surgical technique. In this context, radiomics analysis of the solid enhancing portion of lesions is promising for presurgical diagnosis. Our study found neural networks and then random forest models to be more accurate than other machine learning approaches. Further prospective studies with a larger sample size are needed before the clinical adaptation of radiomics for this application.

Declarations

Funding: The authors declare that no funds, grants, or other support were received during the preparation of this manuscript.

Competing Interests: The authors have no relevant financial or non-financial interests to disclose.

Author Contributions:

All authors contributed to the study conception and design. Material preparation, data collection and analysis were performed by Houman Sotoudeh, Zahra Saadatpour, Ali Rezaei, Mahsan Sotoudeh, Chalres A. Wheeler, Aparna Singhal, and Manoj Tanwar. The first draft of the manuscript was written by Houman Sotoudeh and all authors commented on previous versions of the manuscript. All authors read and approved the final manuscript.

Data Availability: The datasets generated during and/or analysed during the current study are available from the corresponding author on reasonable request.

Ethics approval: This study was performed in line with the principles of the Declaration of Helsinki. Approval was granted by the Ethics Committee of University of Alabama at Birmingham (Record Number IRB-120719006).

Acknowledgement: N/A

References

1. Davis FG, McCarthy BJ (2000) Epidemiology of brain tumors. Curr Opin Neurol 13:635–640. doi:10.1097/00019052-200012000-00004

2. Poretti A, Meoded A, Huisman TA (2012) Neuroimaging of pediatric posterior fossa tumors including review of the literature. J Magn Reson Imaging 35:32–47. doi:10.1002/jmri.22722
3. Lonser RR, Glenn GM, Walther M, Chew EY, Libutti SK, Linehan WM, Oldfield EH (2003) von Hippel-Lindau disease. Lancet 361:2059–2067. doi:10.1016/S0140-6736(03)13643-4
4. Neumann HP, Eggert HR, Weigel K, Friedburg H, Wiestler OD, Schollmeyer P (1989) Hemangioblastomas of the central nervous system. A 10-year study with special reference to von Hippel-Lindau syndrome. J Neurosurg 70:24–30. doi:10.3171/jns.1989.70.1.0024
5. Sora S, Ueki K, Saito N, Kawahara N, Shitara N, Kirino T (2001) Incidence of von Hippel-Lindau disease in hemangioblastoma patients: the University of Tokyo Hospital experience from 1954-1998. Acta Neurochir (Wien) 143:893–896. doi:10.1007/s007010170019
6. Kim EH, Moon JH, Kang SG, Lee KS, Chang JH (2020) Diagnostic challenges of posterior fossa hemangioblastomas: Refining current radiological classification scheme. Sci Rep 10:6267. doi:10.1038/s41598-020-63207-0
7. Pencalet P, Maixner W, Sainte-Rose C, Lellouch-Tubiana A, Cinalli G, Zerah M, Pierre-Kahn A, Hoppe-Hirsch E, Bourgeois M, Renier D (1999) Benign cerebellar astrocytomas in children. J Neurosurg 90:265–273. doi:10.3171/jns.1999.90.2.0265
8. Feletti A, Marrone F, Barresi V, Sala F (2021) Hemangioblastoma with Contrast-Enhanced Cystic Wall: When the Surgical Rule Must Not Be Respected. World Neurosurg 149:190–194. doi:10.1016/j.wneu.2021.02.111
9. Baggenstos MA, Butman JA, Oldfield EH, Lonser RR (2007) Role of edema in peritumoral cyst formation. Neurosurg Focus 22:E9. doi:10.3171/foc.2007.22.5.10
10. Jagannathan J, Lonser RR, Smith R, DeVroom HL, Oldfield EH (2008) Surgical management of cerebellar hemangioblastomas in patients with von Hippel-Lindau disease. J Neurosurg 108:210–222. doi:10.3171/JNS/2008/108/2/0210
11. Greuter L, Guzman R, Soleman J (2021) Typical Pediatric Brain Tumors Occurring in Adults-Differences in Management and Outcome. Biomedicines 9. doi:10.3390/biomedicines9040356
12. Johnson DR, Brown PD, Galanis E, Hammack JE (2012) Pilocytic astrocytoma survival in adults: analysis of the Surveillance, Epidemiology, and End Results Program of the National Cancer Institute. J Neurooncol 108:187–193. doi:10.1007/s11060-012-0829-0
13. Juraschka K, Taylor MD (2019) Medulloblastoma in the age of molecular subgroups: a review. J Neurosurg Pediatr 24:353–363. doi:10.3171/2019.5.PEDS18381
14. Tabatabaei M, Razaei A, Sarrami AH, Saadatpour Z, Singhal A, Sotoudeh H (2021) Current Status and Quality of Machine Learning-Based Radiomics Studies for Glioma Grading: A Systematic Review. Oncology 99:433–443. doi:10.1159/000515597
15. Fedorov ABR, Kalpathy-Cramer J, Finet J, Fillion-Robin J-C, Pujol S, Bauer C, Jennings D, Fennessy F, Sonka M, Buatti J, Aylward SR, Miller JV, Pieper S, Kikinis R (2012) 3D Slicer as an Image Computing Platform for the Quantitative Imaging Network. Magn Reson Imaging Nov 30(9):1323–1341

16. van Griethuysen JJM, Fedorov A, Parmar C, Hosny A, Aucoin N, Narayan V, Beets-Tan RGH, Fillon-Robin JC, Pieper S, Aerts HJWL (2017) Computational Radiomics System to Decode the Radiographic Phenotype. Cancer Res 77(21):e104–e107
17. Demsar JCT, Erjavec A, Gorup C, Hocevar T, Milutinovic M, Mozina M, Polajnar M, Toplak M, Staric A, Stajdohar M, Umek L, Zagar L, Zbontar J, Zitnik M, Zupan B (2013) Orange: Data Mining Toolbox in Python. J Mach Learn Res 14(Aug):2349–2353
18. Shih RY, Smirniotopoulos JG (2016) Posterior Fossa Tumors in Adult Patients. Neuroimaging Clin N Am 26:493–510. doi:10.1016/j.nic.2016.06.003
19. Park DM, Zhuang Z, Chen L, Szerlip N, Maric I, Li J, Sohn T, Kim SH, Lubensky IA, Vortmeyer AO, Rodgers GP, Oldfield EH, Lonser RR (2007) von Hippel-Lindau disease-associated hemangioblastomas are derived from embryologic multipotent cells. PLoS Med 4:e60. doi:10.1371/journal.pmed.0040060
20. Lonser RR, Vortmeyer AO, Butman JA, Glasker S, Finn MA, Ammerman JM, Merrill MJ, Edwards NA, Zhuang Z, Oldfield EH (2005) Edema is a precursor to central nervous system peritumoral cyst formation. Ann Neurol 58:392–399. doi:10.1002/ana.20584
21. Stuer C, Vilz B, Majores M, Becker A, Schramm J, Simon M (2007) Frequent recurrence and progression in pilocytic astrocytoma in adults. Cancer 110:2799–2808. doi:10.1002/cncr.23148
22. Tamilchelvan P, Boruah DK, Gogoi BB, Gogoi R (2021) Role of MRI in Differentiating Various Posterior Cranial Fossa Space-Occupying Lesions Using Sensitivity and Specificity: A Prospective Study. Cureus 13:e16336. doi:10.7759/cureus.16336
23. Payabvash S, Aboian M, Tihan T, Cha S (2020) Machine Learning Decision Tree Models for Differentiation of Posterior Fossa Tumors Using Diffusion Histogram Analysis and Structural MRI Findings. Front Oncol 10:71. doi:10.3389/fonc.2020.00071

Tables

Table 1. The performance of different machine learning models to differentiate PA from HB. AUC: Area Under the Curve.

Model	AUC	Accuracy	Sensitivity	Specificity
Neural Network	0.905	0.82	80	85.1
Random Forest	0.891	0.82	82.6	82.7
kNN	0.868	0.84	86.3	83.3
SVM	0.854	0.8	81.8	80
Naive Bayes	0.835	0.8	86.9	84.6
AdaBoost	0.835	0.76	53.2	59
Decision Tree	0.729	0.73	70.8	75

Figures

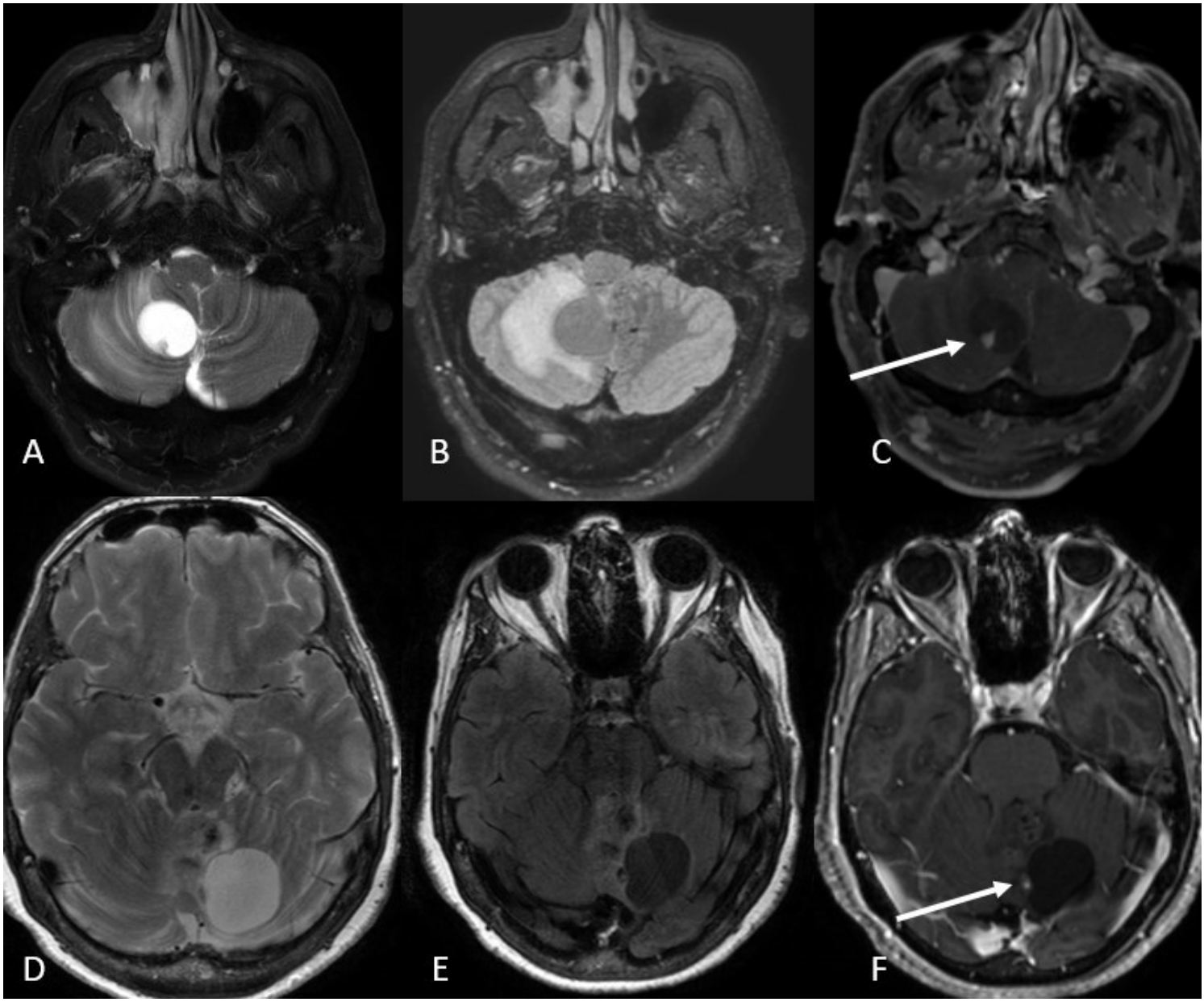

Figure 1

A-C: A hemangioblastoma in the right cerebellar hemisphere in a 29-year-old female presents with a cystic lesion, peripheral edema, and a mural nodule with enhancement (arrow) on post-contrast T1 sequence (A: Axial T2, B: Axial FLAIR, and C: Axial T1 with contrast). D-F: A pilocytic astrocytoma in the left cerebellar hemisphere in a 67-year-old female presents with a cystic lesion, peripheral edema, and a mural nodule with enhancement (arrow) on post-contrast T1 sequence (D: Axial T2, E: Axial FLAIR, and F: Axial T1 with contrast).

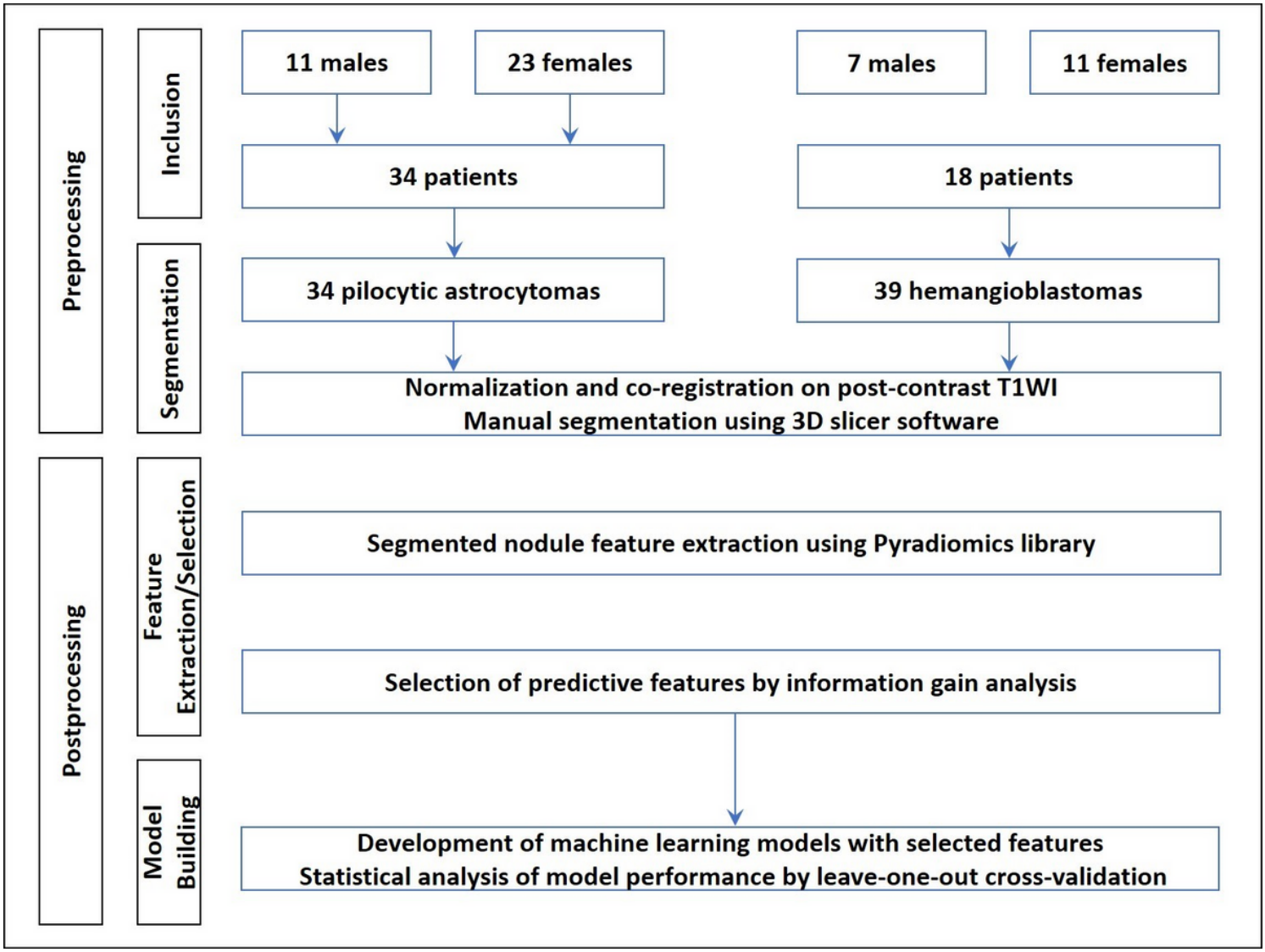

Figure 2

Materials and methods.